Panton-Valentine leukocidin-induced neutrophil extracellular traps lack antimicrobial activity and are readily induced in patients with recurrent PVL^{+}-*Staphylococcus aureus* infections

Short title: PVL induces nontoxic NETs

Authors

Hina Jhelum[1], Dora Čerina[1], CJ Harbort[1], Andreas Lindner[2], Leif Gunnar Hanitsch[3], Rasmus Leistner[4], Jennyver-Tabea Schröder[5], Horst von Bernuth[6,7,8,9], Miriam Songa Stegemann[10], Mariana Schürmann[10], Arturo Zychlinsky[1], Renate Krüger[6*], Gerben Marsman[1*#]

[*] Contributed equally to the manuscript

[#] Corresponding author: marsman@mpiib-berlin.mpg.de

Author affiliations

[1]Department of Cellular Microbiology, Max Planck Institute for Infection Biology, Charitéplatz 1, 10117, Berlin, Germany

[2]Institute of Tropical Medicine and International Health, Charité, Universitätsmedizin Berlin, Berlin, Germany

[3]Department of Medical Immunology, Charité, Universitätsmedizin Berlin, Berlin, Germany

[4]Institute of Hygiene and Environmental Medicine, Charité, Universitätsmedizin Berlin, Berlin, Germany

[5]Department of Pediatric Surgery, Charité, Universitätsmedizin Berlin, Berlin, Germany

[6]Department of Pediatric Respiratory Medicine, Immunology and Critical Care Medicine, Charité - Universitätsmedizin Berlin, corporate member of Freie Universität Berlin, Humboldt-Universität zu Berlin, and Berlin Institute of Health (BIH), Berlin, Germany

[7]Department of Immunology, Labor Berlin GmbH, Berlin, Germany

[8]Berlin Institute of Health at Charité - Universitätsmedizin Berlin, Germany

[9]Berlin-Brandenburg Center for Regenerative Therapies (BCRT), Berlin Institute of Health at Charité, Universitätsmedizin Berlin, corporate member of Freie Universität Berlin, Humboldt-Universität zu Berlin, and Berlin Institute of Health (BIH), Berlin, Germany

[10]Department of Infectious Diseases and Respiratory Medicine, Charité, Universitätsmedizin Berlin, Berlin, Germany

Abstract

Staphylococcus aureus (*S. aureus*) strains that produce the toxin Panton-Valentine leukocidin (PVL; PVL-SA) frequently cause recurrent skin and soft tissue infections (SSTI). PVL binds to and kills human neutrophils, resulting in the formation of neutrophil extracellular traps, but the pathomechanism has not been extensively studied. Furthermore, it is unclear why some individuals colonized with PVL-SA suffer from recurring infections whereas others are asymptomatic. We thus aimed to (a) investigate how PVL exerts its pathogenicity on neutrophils and (b) identify factors that could help to explain the predisposition of patients with recurring infections.

We provide genetic and pharmacological evidence that PVL-induced NET formation is independent of NADPH-oxidase and reactive oxygen species (ROS) production. Moreover, through NET proteome analysis we identified that the protein content of PVL-induced NETs is different from NETs induced by mitogen or the microbial toxin nigericin. The abundance of the proteins cathelicidin (CAMP), elastase (NE), and proteinase 3 (PRTN3) was lower on PVL-induced NETs, and as such they were unable to kill *S. aureus.* Furthermore, we found that neutrophils from affected patients express higher levels of CD45, one of the PVL receptors, and are more susceptible to be killed at a low PVL concentration than control neutrophils. Neutrophils from patients that suffer from recurring PVL-positive infections may thus be more sensitive to PVL-induced NET formation, which might impair their ability to combat the infection.

Importance

Individuals colonized by *Staphylococcus aureus* strains that produce Panton-Valentine leukocidin (PVL-SA) often present with recurrent skin and soft-tissue infections, whilst other individuals remain asymptomatic. PVL is a toxin that kills neutrophils, which results in the formation of neutrophil extracellular traps. Traps induced by other stimuli are known to be toxic to *S. aureus.* We found however that NETs specifically induced by PVL are not toxic to *S. aureus*. Furthermore, we show that neutrophils from individuals that suffer from recurring PVL-SA infections are more sensitive to PVL-induced NET formation compared to healthy individuals. The significance of our work is in identifying a mechanism through which PVL-SA may actively counter the engagement of neutrophils. Moreover, we identified that patients with recuring PVL-SA infections may be more sensitive to this mechanism, which may help to explain their clinical condition and might provide avenues for future treatment development.

Introduction

S. aureus is a widespread Gram-positive pathogen that causes infections in skin and soft tissue (SSTI), osteoarticular, airway, and the blood stream in humans and animals. Nasal colonization with *S. aureus* is found in up to 50% of humans, with strong age variation, and may be asymptomatic provided that skin and mucous membrane barriers are intact [1,2].

93 Pathogenicity of *S. aureus* strains depends on a variety of virulence
94 factors, among those, pore-forming leukocidins such as PVL that target
95 neutrophils (also called polymorphonuclear leukocytes, PMN), and
96 macrophages to evade phagocytosis and intracellular killing (reviewed in
97 [3]). Over the last two decades an increasing number of outbreaks of
98 SSTI in close communities [4–12] and in other health care settings
99 [13,15,14,16–24] were caused by *S. aureus* strains that produce PVL
100 (PVL-SA).

101 Although recurrent skin abscesses and furunculosis are often associated
102 with PVL-SA infections, other pathologies are also linked to these strains.
103 These include (a) worldwide reports of severe invasive infections - often
104 complicated by thrombotic events - in previously healthy young
105 individuals [25–27], (b) breast abscesses in lactating women [28] and
106 transmission to offspring with life-threatening infections [29], and (c)
107 necrotizing pneumonia [30], a severe manifestation, often fatal within
108 days of hospital admission [31,32]. In most cases, pneumonia is preceded
109 by viral airway infections, like influenza, parainfluenza [31,32] and SARS-
110 CoV2 [33,35,34].

111 During outbreaks, identical PVL-SA strains have been obtained from
112 individuals with asymptomatic nasal colonization as well as from patients
113 with severe SSTI or invasive infections [11], suggesting that host factors
114 may explain susceptibility to, and severity of, PVL-SA infections. Although
115 studies in African Pygmies suggest that genetic variations in *C5ARI* may

116 be associated with PVL-SA colonization [36], other factors that allow PVL-
117 SA colonization or infections are not known.

118 The binding specificity of PVL defines both its host- and cell tropism. PVL
119 is a two-component toxin consisting of LukF-PV and LukS-PV, which bind
120 to the human panleukocyte receptor CD45 [37], and the human
121 complement 5a receptors CD88/C5aR and C5L2, respectively [38]. As a
122 result, human phagocytes are the major target of PVL. Upon binding, the
123 subcomponents hetero-oligomerize into an octameric membrane spanning
124 pore [39,40], which drives cell death. Neutrophils express higher levels of
125 both C5a receptors than monocytes [38] and are more sensitive to PVL
126 mediated killing than both monocytes and macrophages [41], suggesting
127 they are the major target of PVL. Importantly, neutrophils are essential
128 for host defense against *S. aureus* [42] and patients with impaired
129 production of reactive oxygen species (ROS) in phagocytes are particularly
130 sensitive to *S. aureus* infections (see review [43]). Neutrophils clear
131 invading *S. aureus* through phagocytosis and by undergoing NETosis, a
132 cell death process which results in the formation of neutrophil extracellular
133 traps (NETs). NETs consist of an externalized web of chromatin decorated
134 with antimicrobial peptides and proteases and are toxic to bacteria [44].

135 Depending on the stimulus, NET formation may require ROS formation
136 [45]. A common mediator of ROS-dependent NET formation is NADPH-
137 oxidase, which produces superoxide (O^{2-}) that spontaneously dismutates
138 to hydrogen peroxide (H_2O_2). Myeloperoxidase (MPO) converts hydrogen
139 peroxide into highly reactive hypochlorous acid (HOCl). ROS production

140 allows for the release of neutrophil proteases from granules, protease-
141 mediated chromatin decondensation and the final lysis of the plasma
142 membrane [46–48]. Two *S. aureus* toxins that kill neutrophils and result
143 in NET formation are γ-hemolysin AB and PVL [49–51]. Interestingly, *S.*
144 *aureus* also produces nucleases to escape from NETs [52]. Whether NET
145 formation is a beneficial or detrimental neutrophil response, both for the
146 host as well as for *S. aureus*, remains unclear and may be context
147 dependent [50].

148 In this study, we set out to characterize PVL-induced NET formation with
149 the aim to understand its possible contribution to the pathogenesis of PVL-
150 SA infections. We show that PVL-induced NET formation is NADPH-oxidase
151 independent. Consistently, neutrophils isolated from chronic
152 granulomatous disease (CGD) patients, which have a mutation in the gene
153 encoding one subunit of the NADPH oxidase complex, make NETs in
154 response to this toxin [53]. PVL-induced NETs showed quantitative
155 proteomic differences to NETs produced after PMA or nigericin stimulation.
156 PVL-NETs contained a lower abundance of multiple antimicrobial proteins
157 and in contrast to PMA- or nigericin-NETs, did not kill *S. aureus.* Given the
158 lack of antimicrobial activity, we asked whether neutrophils from patients
159 with a history of recurrent PVL-SA infection show altered sensitivity to PVL
160 compared to controls. Indeed, we found that neutrophils from these
161 patients express higher levels of the PVL receptor CD45 than healthy
162 controls and make more NETs in response to a low concentration of PVL.
163 Our results suggest that PVL-receptor expression may mediate

164 susceptibility to symptomatic *S. aureus* infection and that NET-formation
165 induced by this toxin serves as an offensive strategy to preemptively
166 neutralize the neutrophil.

167

168

169 **Results**

170 **PVL induces NETs independent from ROS**

171 To further our understanding of the role of PVL toxin in PVL-SA
172 pathogenesis, we verified [50,51] and further characterized PVL-induced
173 NET formation. NADPH-oxidase dependent superoxide formation is
174 essential in NETs induced by some stimuli [45], prompting us to
175 investigate the NETosis pathway initiated by PVL. We first tested
176 superoxide generation in healthy primary neutrophils stimulated with
177 different concentrations of PVL or PMA, a well characterized mitogen that
178 induces NADPH-oxidase dependent NETosis [54]. PVL stimulation resulted
179 in weak superoxide production at all concentrations (Fig 1A). In contrast,
180 PMA induced a significant superoxide burst.

181 We quantified ROS production as well as NET formation in neutrophils
182 from CGD patients. As expected, CGD neutrophils failed to generate
183 superoxide in response to PVL or PMA (Fig 1B). However, unlike PMA, PVL
184 induced extracellular DNA release (Fig 1C) and NET formation (Fig 1D and
185 S1-S8 movies) in CGD neutrophils. These data show that while PVL

186 stimulation weakly activates NADPH-oxidase, NET formation is

187 independent from the produced ROS.

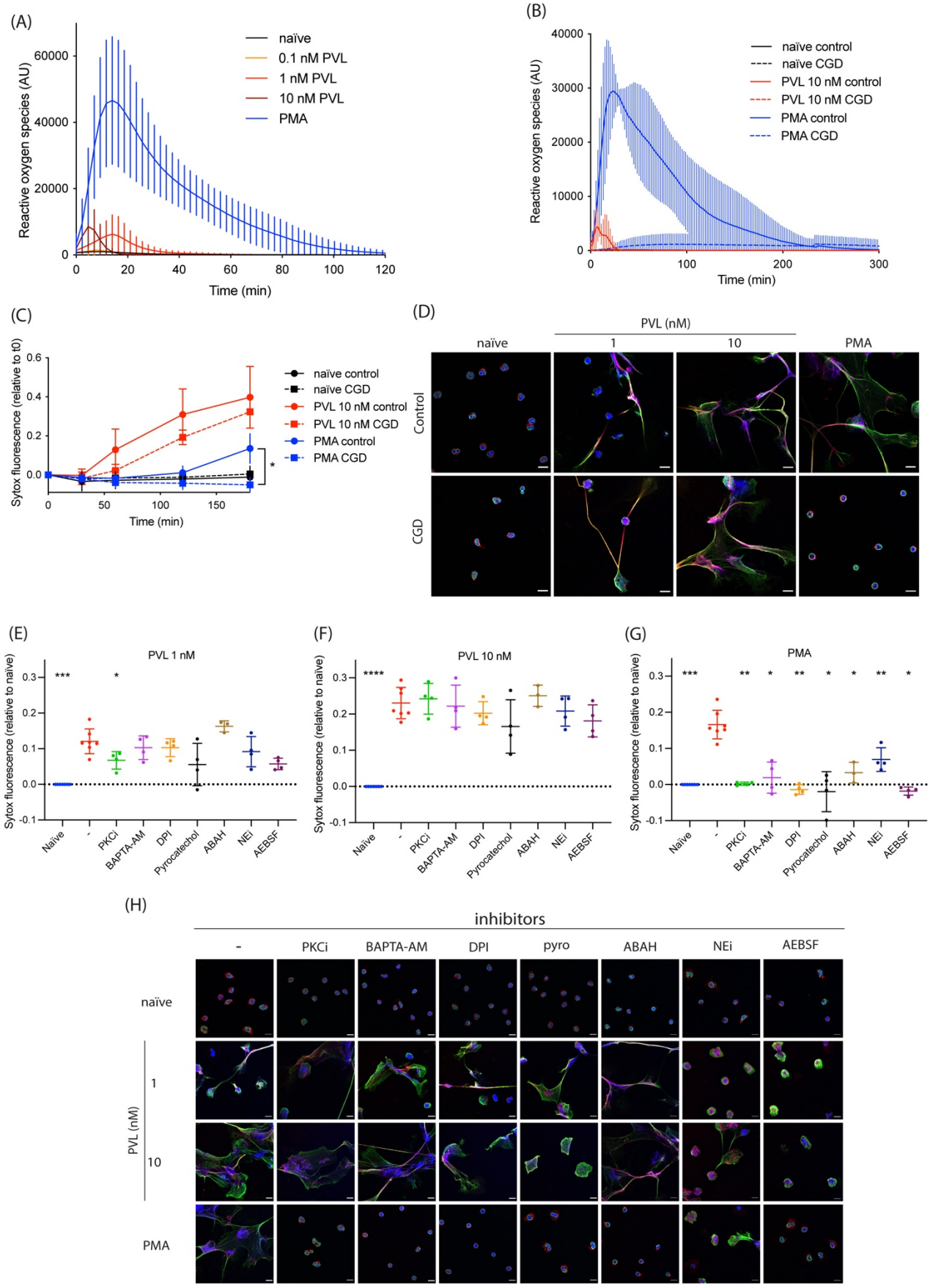

Fig 1. PVL induces ROS-independent NET formation. (A-B) Reactive oxygen species (ROS) formation was quantified in control (A n=14, B n=3) or CGD human primary

191 neutrophils (n=3) stimulated with PMA (50 nM) or PVL (0.1 nM, 1 nM or 10 nM). (C)
192 Control or CGD neutrophils (n=3) were stimulated with PMA (50 nM) or PVL (10 nM) for
193 3h and cell death was quantified using the cell impermeable DNA dye SYTOX Green.
194 Indicated is SYTOX Green fluorescence relative to *t* = 0 min. (D) Representative confocal
195 microscopy images of control and CGD patient neutrophils either naïve or stimulated with
196 PMA (50 nM) or PVL (1 nM or 10 nM) and stained for DNA (blue), NE (red) and chromatin
197 (green). Scale bar represents 10 µm. (E-G) Healthy human neutrophils were treated with
198 PKC inhibitor Gö6983 (PKCi, 1 μM), BAPTA-AM (10 μM), DPI (1 μM), pyrocatechol (30
199 μM), ABAH (500 μM), NEi (20 μM) and AEBSF (100 μM) for 30 min, before stimulating
200 with (E) PVL 1 nM, (F) PVL 10 nM or (G) PMA 50 nM for 4h. We quantified cell death with
201 SYTOX Green and the fluorescence signal relative to naïve is indicated. (H)
202 Representative confocal microscopy of naïve neutrophils or after stimulation with PMA or
203 PVL (1 nM or 10 nM) in the presence or absence of indicated inhibitors, and stained for
204 DNA (blue), NE (red) and chromatin (green). Scale bar represents 10 µm. (C) Two-way
205 ANOVA with Tukey's post-hoc test. *$P<0.05$. (E-G) Mean ±SD of four independent
206 experiments. *$P<0.05$, ** $P<0.01$, *** $P<0.001$, one-way ANOVA with Dunnett´s
207 multiple comparison test.

208 Given the known involvement of various neutrophil proteins in NET
209 formation, we asked if PVL-induced NET formation could be blocked
210 pharmacologically by the PKC inhibitor Gö6983 (PKCi), the calcium
211 chelator BAPTA-AM, the NADPH-oxidase inhibitor DPI, the ROS scavenger
212 pyrocatechol, the myeloperoxidase inhibitor ABAH, the neutrophil elastase
213 inhibitor NEi, or the pan serine protease inhibitor AEBSF (Fig 1E-F and
214 1H). We observed that PKCi weakly inhibited NET formation induced by 1
215 nM PVL (Fig 1E), whilst none of the other inhibitors, including inhibitors of
216 ROS-producing enzymes (DPI and ABAH) or ROS scavengers
217 (pyrocatechol), blocked NET formation induced by 1 or 10 nM PVL (Fig 1E-

218 F and 1H). Notably, neutrophils pre-treated with NEi or AEBSF and
219 stimulated with 1nM PVL formed smaller NETs (Fig 1H). These data
220 suggest that PVL-mediated NET formation is ROS- and protease-
221 independent. As a control, we confirmed [45] that PMA-induced NET
222 formation was blocked by all inhibitors tested (Fig 1G-H).

223 Mazzoleni *et al.* [51] suggested that small conductance calcium-activated
224 potassium (SK) channels and alternative ROS sources, such as
225 mitochondria or xanthine oxidase, mediate PVL-induced NET formation. To
226 verify this, we pre-treated neutrophils with the xanthine oxidase inhibitor
227 allopurinol, the SK channel inhibitor apamin, and the mitochondrial
228 uncouplers DNP and FCCP, before stimulating with either PMA or PVL. The
229 SK channel inhibitor NS8593 was toxic to neutrophils in our hands and
230 was excluded from our experiments. At 1 nM, but not at 10 nM PVL
231 stimulation, allopurinol inhibited NET formation, whilst mitochondrial
232 uncoupling with FCCP partially inhibited NET formation. (S1A-B Fig). These
233 findings were supported by confocal imaging (S1D Fig). None of the
234 inhibitors affected PMA-induced NET formation (S1C Fig). Given that PVL
235 induces NET formation in CGD patients despite a complete lack of ROS
236 (Fig 1B), and the inability of the ROS scavenger pyrocatechol to inhibit
237 PVL-induced NET formation, the inhibition of NETs by allopurinol treatment
238 or mitochondrial uncoupling appears to be independent of ROS production.
239 This is further supported by the observation that DPI, which not only
240 inhibits NADPH-oxidase but all flavin-containing proteins including
241 xanthine oxidase [55] and mitochondrial complex I [56], did not block

242 PVL-induced NET formation (Fig 1E-F). Finally, the inability of ROS-
243 targeting inhibitors to block NET formation induced by 10 nM PVL indicates
244 that PVL-induced NET formation is independent from ROS production.

245

246 **PVL-induced NETs lack enrichment of key antimicrobial proteins**

247 Since PVL induces NETs through a non-canonical pathway we
248 hypothesized that the resulting NETs may have different protein
249 compositions. We therefore analyzed the proteomes of NETs induced by
250 PVL, PMA, and the NADPH-oxidase independent NET inducer nigericin
251 [45]. We analyzed NETs from three independent donors by quantitative
252 mass spectrometry and compared them to the proteome of unstimulated
253 neutrophils. Principal component analysis revealed that PVL-, PMA- and
254 nigericin-induced NETs each have distinct proteomes (Fig 2A).
255 Interestingly, PVL-NETs appear to cluster between naïve neutrophils and
256 NETs induced by PMA and nigericin, suggesting their proteome
257 composition is intermediate between naïve cells and classical NETs.
258 Measurement of the Euclidean distance between samples confirmed that
259 the PVL-NET proteome is less distinct from naïve neutrophils than that of
260 PMA- or nigericin-induced NETs (S2A Fig).

261 We detected 2458 distinct proteins in the combined NET samples (present
262 in at least two of three replicate experiments). To examine which proteins
263 are driving the differences between the NET proteomes, we performed a
264 differential enrichment analysis using a 2-fold change in protein

265 abundance with an adjusted *p* value below 0.01 as a cut-off. We found
266 significant differences in relative protein abundance between all three NET
267 stimuli when compared with naïve neutrophils (Fig 2B and S2A Fig). Fewer
268 differentially abundant proteins (DAPs) were detected between PVL-
269 induced NETs and naïve PMNs (194 significant) compared to PMA- (449)
270 and nigericin-induced NETs (670). These data suggest that the specific
271 enrichment or depletion of proteins during NET formation is lower or
272 incomplete in PVL-treated neutrophils.

273

274

275

276

277

278

279

280

281

282

283

284

285

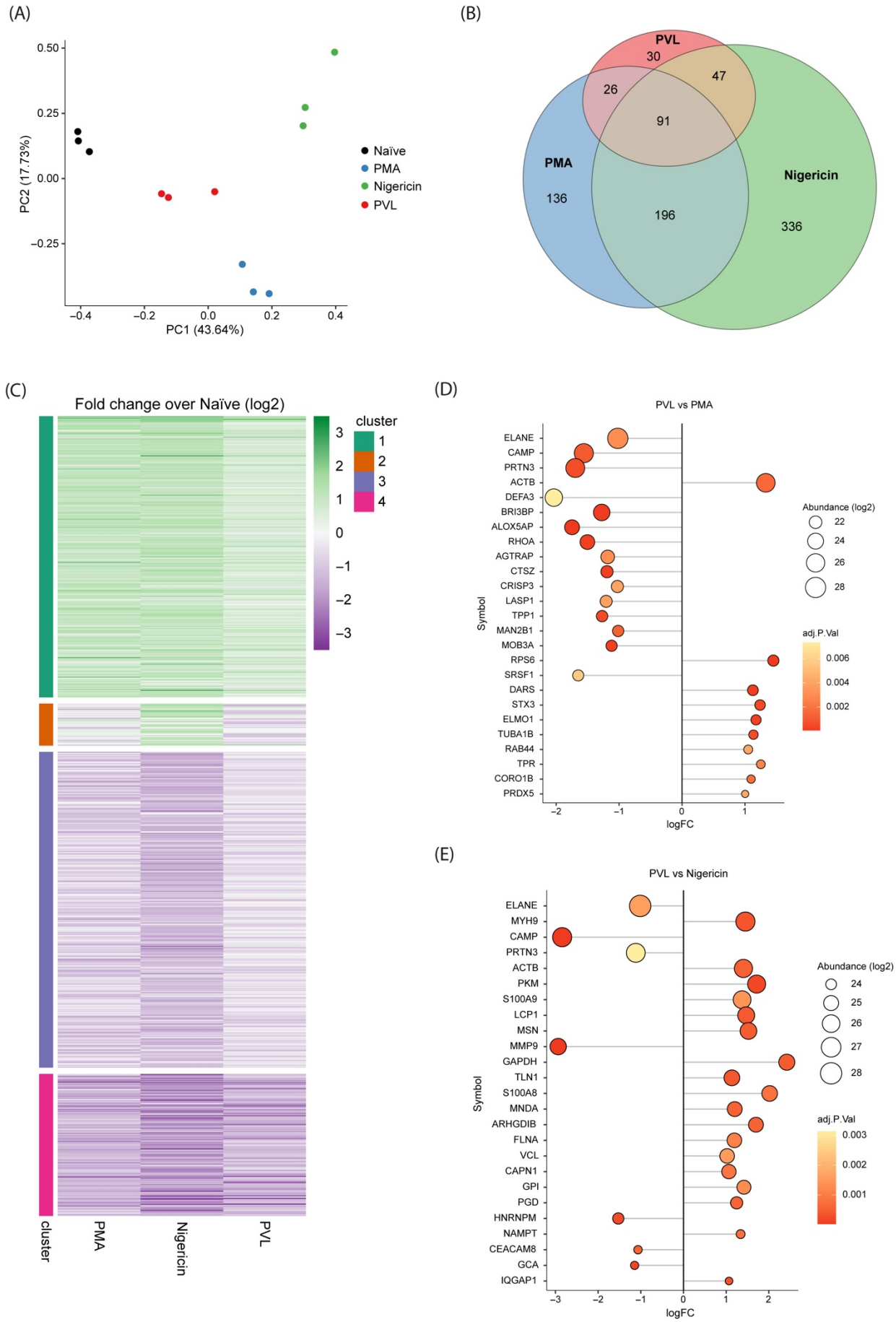

Fig 2. NET proteome assembly is different in PVL-induced NETs. (A) Principal component analysis of the proteomes of naïve neutrophils, and PVL-, PMA-, and

306 nigericin-induced NETs. Analysis was performed on scaled log2-abundance of all proteins
307 detected in at least 2/3 replicates. (B) Euler diagram showing the number and
308 distribution of significant Differentially Abundant Peptides (logFC > 1, adjusted $p < 0.01$)
309 on NETs compared to naïve neutrophils. Areas are proportional to DAP set size. (C)
310 Clustered heatmap showing fold change (log2) values on each NET sample compared to
311 naïve neutrophils of significant DAPs from (B). Clustering was performed by k-means
312 algorithm with k=4 clusters. (D-E) Top 25 most-abundant DAPs that are significantly
313 differentially abundant on PVL-induced NETs compared with PMA- (D) and nigericin-
314 induced NETs (E). Point size and fill color represent average abundance across samples
315 and adjusted *p* value, respectively. Proteomes were made from n=3 samples per
316 condition from independent donors. DAP significance for each comparison was
317 determined by a threshold of |[log2 fold change]| > 1 and adjusted *p* value < 0.01.

318 Examination of the fold changes of NET-specific DAPs revealed that most
319 DAPs have the same pattern of enrichment or depletion across all types of
320 NETs compared to naïve neutrophils (459 with negative logFC, 294
321 positive logFC, Fig 2C). Regression of global DAP fold changes (Fig S2B)
322 revealed that though most proteins have the same enrichment pattern
323 across NETs, the fold-changes are reduced in PVL- compared to PMA- and
324 nigericin-induced NETs (slopes = 0.64, and 0.49 respectively), while PMA
325 and nigericin NETs have equivalent DAP fold-changes (slope = 1).

326 K-means clustering of DAP fold change patterns supported this trend, and
327 further identified a cluster of proteins specifically enriched on nigericin
328 induced NETs (Fig 2C cluster two, orange, and S1 Table). To look more
329 closely at the differences between PVL-induced NETs and PMA- or
330 nigericin-induced NETs, we performed pair-wise comparisons between PVL
331 and PMA or PVL and nigericin (Fig S2C and S2D) and ranked the 25 most

332 abundant DAPs (Fig 2D and 2E, respectively). Among these, key
333 neutrophil proteins such a NE (ELANE), PRTN3, and CAMP, were all less
334 abundant on PVL-induced NETs compared with PMA- or nigericin-induced
335 NETs. In contrast, we found cytoskeleton proteins such as actin (ACTB),
336 myosin (MYH9), and tubulin (TUBA1B) to be more enriched on PVL-NETs.
337 Our data suggest that PVL induces NETs with a different NET proteome
338 assembly when compared with PMA or nigericin, resulting in a lack of
339 enrichment of key antimicrobial proteins on PVL-NETs.

340

341 **PVL-induced NETs are less bactericidal**

342 Given the differential enrichment of antimicrobial proteins in PVL-
343 compared to PMA- and nigericin-NETs, we hypothesized that their
344 bactericidal activity may be different. We incubated methicillin-resistant *S.*
345 *aureus* (MRSA) with either PVL-, PMA-, or nigericin-induced NETs for 1 h,
346 harvested the bacteria, and quantified the surviving colony forming units.
347 PVL-induced NETs did not kill MRSA, whilst PMA- and nigericin-induced
348 NETs did (Fig 3A). We verified that all stimuli at these concentrations
349 released similar amounts of NETs by nanodrop DNA quantification (Fig
350 3B). To exclude a possible contribution of killing through phagocytosis we
351 performed the same experiment in the presence of cytochalasin B. We did
352 not observe a difference in antimicrobial activity upon inhibition of
353 phagocytosis, indicating that NETs were solely responsible for the killing
354 (Fig S3). These results show that PVL-NETs have a lower antimicrobial
355 potential against MRSA than PMA- or nigericin-NETs.

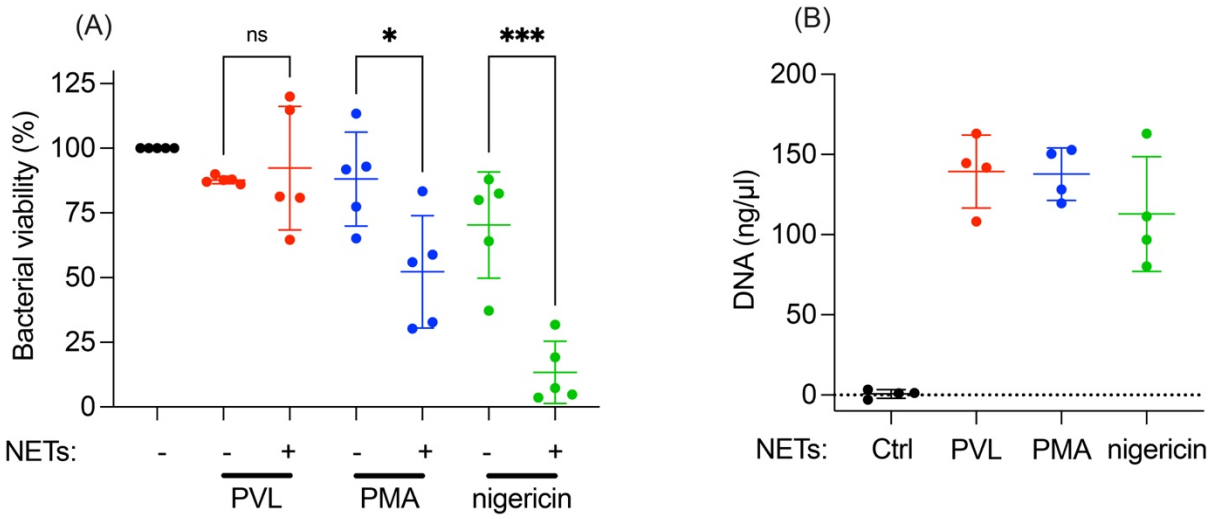

Fig 3. PVL-induced NETs do not kill MRSA. (A) Primary human neutrophils were stimulated with PVL (100 nM), PMA (100 nM), or nigericin (30 µM), for 4 h to induce NETs. MRSA was incubated with NETs for 1 h and CFU was quantified. Bacterial viability is expressed as a percentage of CFUs normalized to MRSA incubated in the absence of NETs. (B) The DNA content of PVL-, PMA-, and nigericin-induced NETs at 4 h was quantified by spectrophotometry. (A) Mean ± SD of five independent experiments. *$p<0.05$, *** $p<0.001$, one-way ANOVA. (B) Mean ± SD of four independent experiments.

PVL induces NETs efficiently in neutrophils from patients with recurrent PVL-SA infections

The lack of antimicrobial activity of PVL-NETs prompted us to ask whether neutrophils from patients that suffer from recurrent PVL-SA infections show altered responses to PVL that may help to explain the patients' increased susceptibility to infection. We quantified NET formation in response to 0.1 nM, 1 nM, and 10 nM PVL in patients and controls using a cell impermeable DNA dye. Interestingly, 0.1 nM PVL killed neutrophils isolated from patients more efficiently than neutrophils isolated from

380 healthy controls (Fig 4A). Patient and control neutrophils were equally
381 susceptible to make NETs in response to PMA.

382 Given the binding specificity of PVL we checked the expression of CD45,
383 CD88, and C5L2, as well as the neutrophil activation markers CD63 and
384 CD66b on control and patient neutrophils by flow cytometry. Patient
385 neutrophils expressed higher levels of CD45 (adjusted *p* value =
386 0.000473), and there was no difference in CD88. Furthermore, a subset of
387 patients expressed increased C5L2 levels compared to control neutrophils
388 (Fig S4A), but this trend was not consistent for all patients (Fig 4B).
389 Interestingly, the difference in expression of C5L2 and possibly CD45 in
390 patients compared to controls correlated with the difference in NET
391 formation in response to 0.1 nM PVL (ρ = 0.4491 for CD45, ρ = 0.7105 for
392 C5L2) (Fig 4C and 4D). Differences in expression levels of CD88, CD63 or
393 CD66b did not correlate with differences in NET formation (Fig S4B-D).

394 Taken together, our data suggest that neutrophils from patients with
395 recurrent PVL-SA infections express higher levels of the PVL receptor
396 CD45 and may be more sensitive to PVL-induced NET formation at low
397 PVL concentrations when compared to control neutrophils.

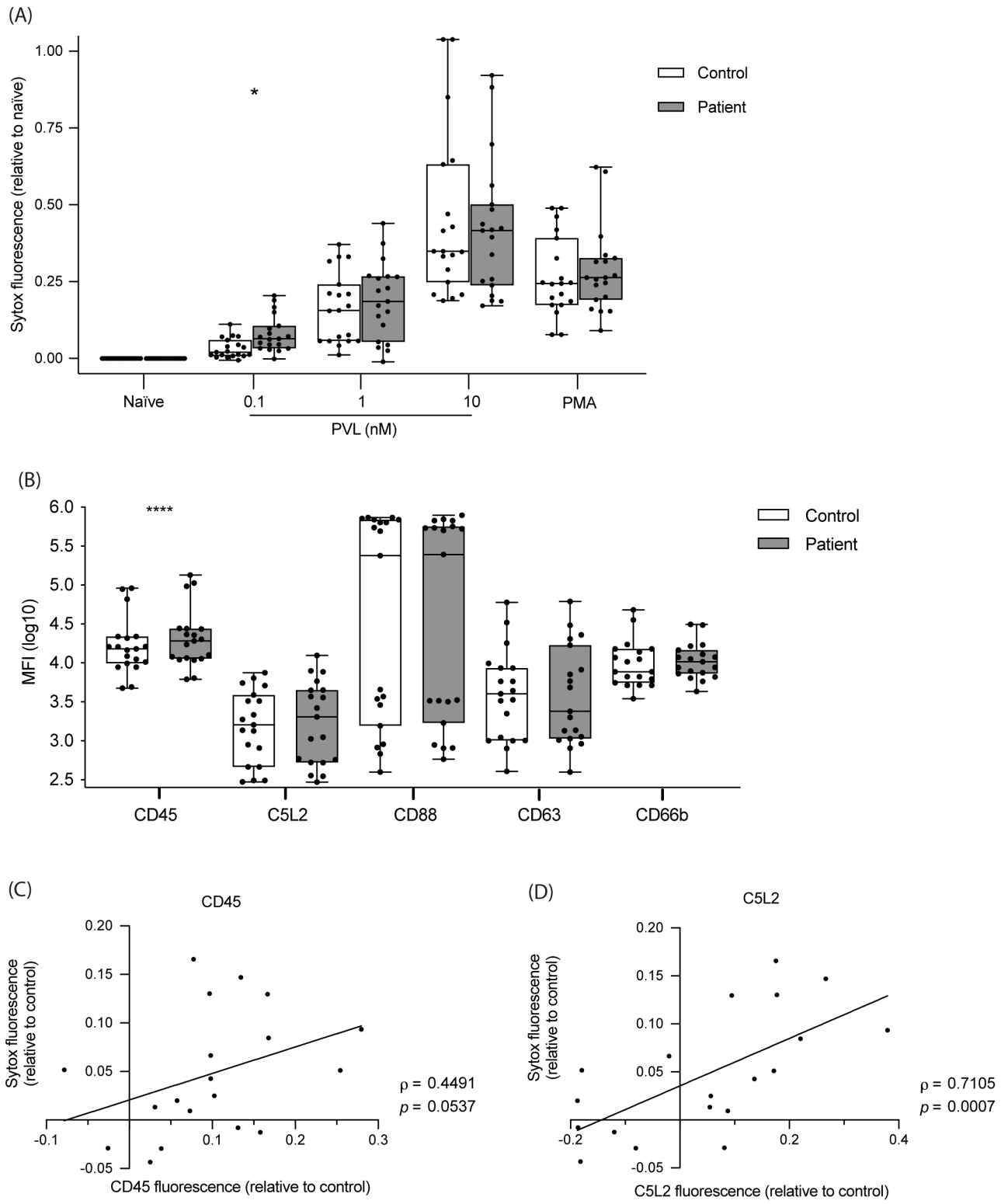

Fig 4. Neutrophils from patients with recurrent PVL-SA infections make more NETs in response to PVL and express more CD45 than neutrophils from healthy donors. (A) Purified primary neutrophils from patients suffering from recurrent PVL-SA infections (n=19) and healthy controls (n=19) were either left untreated or stimulated with PMA (50 nM) or PVL (0.1 nM, 1 nM or 10 nM) for 4 h and cell death was quantified

404 by adding the cell-impermeable DNA dye SYTOX Green and measuring fluorescence.
405 Boxplot indicates SYTOX fluorescence relative to naïve neutrophils at 4 h. (B) CD45,
406 C5L2, CD88, CD63 and CD66b were immunolabelled on neutrophils from patients and
407 healthy controls. The fluorescence was measured and indicated as log-transformed MFI.
408 (C) CD45 or (D) C5L2 fluorescence of patient neutrophils relative to control was plotted
409 against SYTOX fluorescence of patient neutrophils relative to control after incubation with
410 0.1 nM PVL for 4 h. (A) Unpaired Wilcoxon signed rank test with Bonferroni post-hoc test,
411 * $P<0.05$. (B) Paired *t*-test, *** $P<0.001$. (C-D) Spearman's correlation test where the
412 coefficient of correlation (ρ) and probability (p) are indicated. A best-fit line indicates the
413 trend.

414

415 **Discussion**

416 In the past few decades, PVL has emerged as an important virulence
417 factor in community acquired SA infections. Interestingly, human host
418 factors that mediate susceptibility or severity of PVL-SA infections are not
419 known. To further our understanding of the contribution of PVL to PVL-SA
420 pathogenesis, we set out to characterize PVL-induced NET formation. PMA
421 or *Candida albicans* induce NET formation which is ROS-dependent and is
422 blocked by compounds that scavenge ROS or inhibit ROS [45]. Other
423 stimuli, like nigericin and calcium ionophores induce NETs through a ROS
424 independent mechanism [45]. We identified that PVL induces the
425 formation of NETs independently of NADPH-oxidase and MPO activity, two
426 enzymes that produce ROS. This is evidenced by two observations (1)
427 CGD neutrophils do not produce ROS upon stimulation with PVL, but make
428 NETs, and (2) DPI, an inhibitor of flavin-containing proteins such as

429 NADPH-oxidase, xanthine oxidase [55], and cytochrome C [57,56], the
430 ROS scavenger pyrocatechol, and the MPO inhibitor ABAH all fail to inhibit
431 PVL-induced NET formation.

432 A recent study by Mazzoleni *et al*. suggested that ROS derived from
433 mitochondria or xanthine oxidase are involved in PVL-induced NET
434 formation [51]. We observed that treatment with DNP or FCCP, as well as
435 xanthine oxidase inhibition by allopurinol partly inhibited PVL-induced NET
436 formation. Xanthine oxidoreductase consists of two isoforms, xanthine
437 oxidase and xanthine dehydrogenase. Allopurinol inhibits both isoforms,
438 which affects purine metabolism. Moreover, allopurinol itself generates
439 superoxide radicals upon inhibition of xanthine oxidase [58]. Therefore, its
440 inhibitory effect on PVL-induced NET formation may be independent from
441 xanthine oxidase inhibition or ROS formation. How allopurinol exerts its
442 inhibitory effects on PVL-induced NET formation is still unclear.
443 Furthermore, given that both DPI and the ROS scavenger pyrocatechol
444 were unable to inhibit PVL-induced NET formation, we hypothesize that
445 the inhibitory effect of allopurinol and FCCP is independent from their
446 effects on ROS production. Notably, inhibition of NET formation by these
447 inhibitors was seen at 1 nM PVL but was lost when stimulating with 10 nM
448 PVL. It may be that PVL at high concentrations is able to induce NET
449 formation without the involvement of neutrophil components interrogated
450 by the inhibitors used in our study, whilst at low PVL concentrations some
451 components may contribute to NET formation.

452 Neutrophil proteases were not essential for PVL-induced NET formation,
453 although we did observe that formed NETs appeared smaller upon
454 protease inhibition. Neutrophil elastase is known to contribute to
455 chromatin decondensation during NADPH-oxidase dependent NETosis
456 [47,59] and this decondensation may occur during PVL-mediated NET
457 formation as well. Although PAD4-mediated histone citrullination has been
458 suggested to be involved in NADPH oxidase-independent NET formation,
459 others have excluded its involvement in driving PVL-induced NET
460 formation [51].

461 Interestingly, different NETosis mechanisms lead to NETs with specific
462 compositions. We find differences in protein abundances of NETs induced
463 by PVL, PMA, or nigericin, and the proteome of PVL NETs specifically
464 appears to be less distinct from that of unstimulated neutrophils. Several
465 antimicrobial proteins are less abundant in PVL-induced NETs, when
466 compared to PMA- or nigericin-induced NETs. In contrast, cytoskeletal
467 proteins are more abundant on PVL NETs. A previous report also identified
468 a similar enrichment of cytoskeletal proteins in spontaneously lysed
469 neutrophils [60]. Given PMA or nigericin-induced NET formation involves
470 an intracellular release of granular components [59], this 'mixing-of-the-
471 bag' may allow for efficient tethering of granular components to the
472 chromatin backbone and degradation of the cytoskeleton. Cell lysis occurs
473 2-3 h after stimulation with PMA, while PVL-induced NET formation occurs
474 swiftly, with cell lysis occurring within the first 2 h after stimulation. We
475 speculate that granular components may be lost to the extracellular

476 environment during this rapid lysis, resulting in a less bactericidal NET.
477 These data suggest that NETs induced by different stimuli may display
478 different functional characteristics. Leukocidins such as PVL may have
479 evolved to elicit a harmless form of NET formation to promote survival of
480 the invading bacteria.

481 We hypothesized that the lack of antimicrobial activity of PVL-NETs might
482 contribute to PVL-SA pathogenesis and asked whether neutrophils from
483 patients that suffer from recurrent PVL-SA infections show unusual
484 responses to PVL. We identified increased NET formation in patient
485 neutrophils upon stimulation with a low PVL concentration, and a higher
486 expression of CD45 and potentially C5L2, two of the toxin's receptors, in
487 patient neutrophils compared to healthy controls. Furthermore, the
488 increase in CD45 and C5L2 expression correlated with more NET formation
489 induced by PVL.

490 LukS-PV and LukF-PV have different binding affinities to their respective
491 receptors (C5L2 and CD88 for LukS-PV, CD45 for LukF-PV), and the low
492 binding affinity of LukF-PV to CD45 suggests that varying expression
493 levels of CD45 are unlikely to modulate pore formation [37]. In contrast,
494 LukS-PV binding affinity to CD88 or C5L2 is much higher and therefore
495 their expression may modulate sensitivity to PVL toxin. Given that
496 neutrophils express C5L2 less abundantly than CD88, it was surprising to
497 find that differential expression of C5L2 correlates with an increased
498 sensitivity of patient neutrophils to PVL [38]. However, the affinities of
499 LukS-PV binding to CD88 and C5L2 have never been compared and the

500 relative contribution of C5L2-binding to PVL mediated cell death is
501 therefore not known. Whether there is a genetic predisposition in patients
502 with recurrent PVL-SA remains to be determined and we are currently
503 investigating avenues to study this.

504 CD88 localizes to the plasma membrane, rendering it accessible for
505 extracellular PVL toxin. However, there are conflicting reports on the
506 localization of C5L2 since it has been detected both intracellularly and on
507 the plasma membrane [61,62]. We detected C5L2 on the plasma
508 membrane through flow cytometry, suggesting that the expression is not
509 exclusively intracellular. However, much is unknown concerning the
510 regulation of C5L2 and CD88 expression and receptor shuttling and it is
511 unclear how this regulation might affect targeting by PVL [61,62].

512 Pore formation by PVL is described to exert various cellular effects such as
513 intracellular calcium flux, ATP-release into the extracellular environment,
514 induction of apoptosis and cellular lysis [63]. These various phenotypes
515 likely depend on the toxin concentration a cell encounters. We therefore
516 characterized NET formation at different PVL concentrations and observed
517 robust NET formation upwards of 1 nM PVL. In clinical samples from PVL-
518 SA patients, median levels of PVL toxin were previously found to be
519 0.42μg/ml (~11 nM) with a range of 0-399 μg/ml, which suggests that
520 NET induction may be expected in these patients [64], notwithstanding
521 the difficulty of predicting PVL potency *in vivo*.

522 NETs have at least three described functions, they are antimicrobial [44],
523 procoagulant [65], and activate the immune system [66,67]. PVL-SA

524 infections may be associated with a higher risk for thrombotic events. In
525 addition to being less antimicrobial, it would be interesting to investigate if
526 PVL-induced NETs also differ in their procoagulant or immune activation
527 functions.

528 In conclusion, our observation of (a) differentially expressed PVL receptors
529 in individuals with recurrent or severe PVL-SA infections and (b)
530 functionally different NET formation after neutrophil exposure to PVL in
531 contrast to other stimuli may explain specific clinical features and
532 interindividual differences in PVL-SA infections. We propose that
533 overexpression of PVL receptors might make an individual's neutrophils
534 more prone to this disarmed NET formation, preventing efficient clearance
535 of the invading bacteria. In turn, this could provide a competitive
536 advantage to PVL-SA, facilitating colonization and recurrent infections.
537 Further investigations are necessary to verify this finding and find
538 potential treatment or prevention strategies for these infections.

539

540 Materials and Methods

541 Neutrophil isolation, experimental conditions, and inhibitors

542 Human neutrophils were isolated by layering whole blood over
543 Histopaque-1119 (Sigma) followed by a discontinuous Percoll gradient
544 (Amersham Biosciences) as previously described [46]. Alternatively, they
545 were also isolated using the direct human neutrophil isolation kit
546 (EasySep, StemCell Technologies) following manufacturer´s instructions.

547 All experiments were performed in Seahorse XF RPMI medium (SF-RPMI,
548 Agilent) supplemented with 2 mM glutamine, 10 mM HEPES, 1 mM
549 glucose and 0.1% human serum albumin (HSA) at pH 7.4 except where
550 mentioned. The stimuli used to induce NET formation were phorbol 12-
551 myristate 13-acetate (PMA, Sigma), PVL (equal amounts of *S. aureus*
552 recombinant LukS and LukF (Bioservices), and nigericin (InvivoGen). We
553 used the following inhibitors: Gö6983 (PKCi, Tocris) BAPTA-AM (Thermo
554 Fisher Scientific), pyrocatechol (Sigma), 4-Aminobenzoic acid hydrazide
555 (ABAH, Cayman chemical), neutrophil elastase inhibitor (NEi,
556 MedChemExpress), Diphenyleneiodonium chloride (DPI, Calbiochem),
557 AEBSF (Sigma), allopurinol (Sigma), Apamin (Sigma), 2,4- Dinitrophenol
558 (DNP, Sigma) and 2-[[4-(trifluoromathoxy) phenyl]hydrazinylidene]
559 propanedinitrile (FCCP, Abcam).

560

561 **ROS measurement**

562 Purified neutrophils were seeded at 10^5 cells per well in a 96-well plate
563 and incubated for 30 min with the indicated inhibitors, followed by
564 incubation for 10 min with 50 μM luminol and 1.2 units/ml horseradish
565 peroxidase at 37°C prior to stimulation with indicated stimuli.
566 Luminescence was measured over time in a VICTORX luminometer (Perkin
567 Elmer) [45].

568

569 **Neutrophil lytic cell death assay**

570 10^5 neutrophils were seeded in a 96-well plate and incubated with the
571 appropriate inhibitors for 30 min, followed by incubation with 50 nM cell-
572 impermeable DNA dye SYTOX Green (ThermoFisher Scientific) for 5 min at
573 37°C, prior to stimulation with indicated stimuli. Fluorescence was
574 recorded once per hour for 4h using a Fluoroskan Ascent (ThermoFisher
575 Scientific).

576

577 **NET staining**

578 10^5 neutrophils were seeded on glass coverslips in a 24-well plate and
579 incubated with or without appropriate inhibitors followed by stimulation
580 with indicated stimuli for 4 h at 37°C. Cells were fixed with 4%
581 paraformaldehyde (PFA) for 20 min at room temperature. Cells were
582 washed with PBS, permeabilized with 0.5% Triton X-100 for 1 min and
583 incubated in blocking buffer (3% normal goat serum, 3% cold water fish
584 gelatin, 1% bovine serum albumin and 0.05% Tween-20 in PBS) for 30
585 min. Neutrophils were then stained using antibodies detecting elastase
586 (Merck Millipore, 481001) and a subnucleosomal complex of Histone 2A,
587 histone 2B and chromatin [68]. The secondary antibodies used were goat
588 anti-mouse Alexa Fluor 488 (Invitrogen, A11029) and goat anti-rabbit
589 Alexa Fluor 647 (Invitrogen, A21245) followed by staining with DAPI (0.1
590 μg/ml, Invitrogen). Finally, the samples were mounted using antifade
591 mountant (ProLong Diamond Antifade mountant, ThermoFisher Scientific).
592 Images were acquired using a Leica TCS SP8 confocal microscope.

593 For live NET imaging, cells were resuspended in Agilent XF RPMI medium
594 (Agilent) at pH 7.4, supplemented with 0.1% Human Serum Albumin, 10
595 mM Glucose (Sigma Aldrich), 2 mM L-Glutamine (Gibco), 20 mM HEPES
596 (Gibco) 500 nM SYTOX Green (Thermo Fischer) and 2.5 µM DRAQ5
597 (Biostatus) and seeded at a density of $5x10^5$ cells per well into µ-slide 8
598 well ibiTreat dishes (ibidi). Cells were stimulated with final concentrations
599 of 100 nM PMA and 10 nM PVL. Images were collected at 2 min intervals
600 on a Leica TCS SP8 confocal microscope equipped with a climate chamber
601 at 37°C and with a Leica HC PL APO 20x/0.75 IMM CORR CS2 objective
602 using glycerol immersion [45].

603

604 **Mass spectrometry (MS)**

605 Human neutrophils from three different healthy donors were seeded in 6-
606 well tissue culture plate to a density of $3x10^5$ cells per well (SF-RPMI
607 without HSA) and then stimulated with 50 nM PMA, 10 nM PVL, or 15 µM
608 nigericin for 4 h to induce NETs. As a control, neutrophils were incubated
609 in medium for 4 h. Media was carefully removed followed by a wash with
610 fresh media to remove unbound proteins. NETs were collected by
611 treatment with lysis buffer (1% SDS, 50 mM HEPES pH 8, 10 mM tris-(2-
612 carboxyethyl)phosphine (TCEP), 40 mM Chloroacetamide and protease-
613 inhibitor cocktail) and subsequent scraping.

614 All samples were subjected to SP3 sample preparation [69]. Briefly,
615 proteins were denatured, reduced and alkylated, and subsequently

616 digested with Trypsin and Lys-C proteases. TMT 11plex (Pierce) labelling
617 was used for peptide multiplexing and quantification. Samples were
618 mixed, desalted using solid phase extraction (Seppak 1cc/50 mg, Waters),
619 and fractionated using basic reversed phase fractionation on a quaternary
620 Agilent 1290 Infinity II UPLC system equipped with a Kinetex Evo-C18
621 column (150 x 2.1 mm, 2.6µm, 100 Å, Phenomenex). Fractions were
622 concatenated into 8 final samples, dried down and resuspended in 2%
623 acetonitrile, 0.1% trifluoroacetic acid (TFA) prior MS analysis. All samples
624 were analyzed on an Orbitrap Q Exactive HF (Thermo Scientific) that was
625 coupled to a 3000 RSLC nano UPLC (Thermo Scientific). Samples were
626 loaded on a pepmap trap cartridge (300 µm i.d. x 5 mm, C18, Thermo)
627 with 2% acetonitrile, 0.1% TFA at a flow rate of 20 µL/min. Peptides were
628 separated over a 50 cm analytical column (Picofrit, 360 µm O.D., 75 µm
629 I.D., 10 µm tip opening, non-coated, New Objective) that was packed in-
630 house with Poroshell 120 EC-C18, 2.7 µm (Agilent). Solvent A consists of
631 0.1% formic acid in water. Elution was carried out at a constant flow rate
632 of 250 nL/min using a 180-minute method: 8-33% solvent B (0.1% formic
633 acid in 80% acetonitrile) within 120 minutes, 33-48% solvent B within 25
634 minutes, 48-98% buffer B within 1 minute, followed by column washing
635 and equilibration. The mass spectrometer was operated in data-dependent
636 acquisition mode. The MS1 survey scan was acquired from 375-1500 m/z
637 at a resolution of 120,000. The top 10 most abundant peptides were
638 isolated within a 0.7 Da window and subjected to HCD fragmentation at a
639 normalized collision energy of 32%. The AGC target was set to 2e5

640 charges, allowing a maximum injection time of 78 ms. Product ions were
641 detected in the Orbitrap at a resolution of 45,000. Precursors were
642 dynamically excluded for 45 s. Raw files were processed with Proteome
643 Discoverer 2.3 (Thermo Scientific) using SEQUEST HT for peptide
644 identification. Peptide-spectrum-matches (PSMs) were filtered to a 1%
645 false discovery rate (FDR) level using Percolator employing a target/decoy
646 approach. The protein FDR was set to 1%. Further data processing was
647 carried out in R and Perseus (v. 1.6.2.3). Only proteins identified with at
648 least two peptides were included in the analysis. All contaminant proteins
649 were filtered out. A three-step normalization procedure was applied. First,
650 the total intensity of each TMT channel was normalized to correct for
651 mixing errors. Next, the common channel in both TMT sets was used for
652 internal reference scaling [70] in order to correct for batch effects.
653 Afterwards the data was normalized applying trimmed mean of M values
654 (TMM) using the edgeR package in R [71]. Proteins were filtered on those
655 detected in at least two of three replicate experiments. Remaining
656 undetected (NA) values were replaced with the sample-wise minimum
657 abundance as an estimation of the limit of detection. Differential protein
658 abundances were calculated using the limma package in R [72]. Principle
659 component analysis and calculation of Euclidean distance between
660 proteome samples were performed using scaled log2(abundance) values.

661

662 **NET killing assay**

663 Purified neutrophils were seeded at 10^6 cells per well in a flat-bottom 96-
664 well plate. NET formation was induced with 100 nM PVL, 100 nM PMA or
665 30 µM nigericin for 4 h at 37 °C. If applicable, residual phagocytosis was
666 subsequently blocked with 10 µg/ml cytochalasin B (Abcam) for 15 min.
667 *S. aureus* (USA300) in mid-logarithmic phase was added at a multiplicity
668 of infection of 2 in RPMI with 10% human serum (Sigma). Bacteria were
669 spun down for 5 min at 800 x g and incubated for 1 h at 37 °C. After
670 incubation, NETs were treated with 2 U micrococcal nuclease (Takara Bio)
671 for 10 min at RT. Samples were resuspended, serially diluted in DPBS and
672 plated on trypticase soy agar plates. The plates were incubated overnight
673 at 37 °C and colony-forming units were counted. Bacterial viability was
674 expressed as a percentage of bacteria incubated for 1h without NETs.

675 For DNA quantification, NETs were induced as described above and
676 digested with 2 U micrococcal nuclease for 10 min at RT, and
677 subsequently with 0.5 mg/ml of proteinase K (Invitrogen) for 1 h at 50°C.
678 The samples were vortexed and the DNA concentration was measured on
679 Nanodrop 2000 spectrophotometer (ThermoFisher Scientific).

680

681 **Neutrophil markers**

682 $1x10^6$/ml neutrophils were fixed for 15 min using 4% PFA and washed to
683 PBS supplemented with 0.1% HSA. Cells were incubated with anti-CD63-
684 PE, anti-CD66b-APC (Miltenyi Biotec), 5 µg/ml anti-CD45-AlexaFluor 647
685 (Santa Cruz Biotechnology), 10 µg/ml CD88 (S5/1)-FITC (Santa Cruz

686 Biotechnology) and 10 µg/ml anti-human C5L2-APC (BioLegend)
687 antibodies for 30 min in the dark, washed thereafter to PBS supplemented
688 with 0.1% HSA and measured on a CytoFLEX (BeckMan Coulter) or
689 MACSQuant (Miltenyi Biotec).

690

691 **Patient and control characteristics**

692 Patient demographic and clinical data are summarized in S2 Table.
693 Controls were matched for gender and age. All study participants provided
694 written informed consent and were free of infections at the time of blood
695 withdrawal. The study was approved by the local Ethics committee
696 (EA2/003/19). Healthy control samples were collected according to the
697 approval and guidelines of the local ethics committee (EA1/0104/06).

698

699 **Statistical analysis**

700 Analysis of differential protein abundance was performed in limma (Linear
701 Models for Microarray data) in R, which has been shown to outperform t-
702 tests in detecting significant changes in protein abundance [73]. Protein-
703 wise linear models were fit and batch-corrected using the formula (0 +
704 condition + batch) and significant changes in abundance were tested
705 using an empirical Bayes moderated t-statistic with Benjamini-Hochberg
706 correction. Changes in abundance were considered significant at an
707 absolute log2 fold change > 1, and an adjusted *p* value < 0.01. Euler
708 diagrams of significant changes across samples were visualized with the

709 eulerr package [74]. Significant proteins were clustered by pattern across
710 conditions using k-means clustering with indicated number of clusters.
711 Heatmaps were produced using pheatmap package [75].

712 R scripts for proteome analysis and visualization can be found in the
713 supporting zip document.

714 Data are represented as mean±SD unless otherwise stated.

715

716 **MS data availability**

717 The mass spectrometry proteomics data have been deposited to the
718 ProteomeXchange Consortium via the PRIDE [76] partner repository with
719 the dataset identifier PXD025702.

720 Reviewer account details:

721 **Username:** reviewer_pxd025702@ebi.ac.uk

722 **Password:** Yr3cVMPZ

723

724 **Acknowledgements**

725 We thank Christian Frese from the Proteomics Research Platform at the
726 Max Planck Unit for the Science of Pathogens for proteomic analysis.

727 We thank Alf Herzig for visualizing PVL-induced NET formation in healthy
728 and CGD neutrophils in real time by confocal microscopy.

729

730 **Author Contributions**

731 HJ, AZ, RK, and GM designed the study

732 HJ, DC, and GM performed experiments and analyzed the data

733 HVB and RK cared for the patients

734 AL, LGH, RL, JTS, MSS, MS, and HVB have interpreted the data and
735 revised the manuscript for important intellectual content

736 CJH analyzed the mass spectrometry data

737 HJ, AZ, RK, and GM wrote the manuscript

738

739 **Competing interests**

740 The authors declare that they have no competing interests.

741

742

743 **References**

744 1. Bogaert D, van Belkum A, Sluijter M, Luijendijk A, de Groot R,
745 Rümke H, et al. Colonisation by Streptococcus pneumoniae and
746 Staphylococcus aureus in healthy children. Lancet. 2004;363: 1871–
747 1872. doi:10.1016/S0140-6736(04)16357-5

748 2. Wertheim HFL, Melles DC, Vos MC, van Leeuwen W, van Belkum A,
749 Verbrugh HA, et al. The role of nasal carriage in Staphylococcus
750 aureus infections. Lancet Infect Dis. 2005;5: 751–62.
751 doi:10.1016/S1473-3099(05)70295-4

752 3. Tromp AT, van Strijp JAG. Studying Staphylococcal Leukocidins: A
753 Challenging Endeavor. Front Microbiol. 2020;11: 1–8.
754 doi:10.3389/fmicb.2020.00611

755 4. Müller-Premru M, Strommenger B, Alikadic N, Witte W, Friedrich AW,
756 Seme K, et al. New strains of community-acquired methicillin-
757 resistant Staphylococcus aureus with Panton-Valentine leukocidin
758 causing an outbreak of severe soft tissue infection in a football team.
759 Eur J Clin Microbiol Infect Dis. 2005;24. doi:10.1007/s10096-005-
760 0048-0

761 5. Gilbert M, MacDonald J, Louie M, Gregson D, Zhang K, Elsayed S, et
762 al. Prevalence of USA300 colonization or infection and associated
763 variables during an outbreak of community-associated methicillin-
764 resistant Staphylococcus aureus in a marginalized urban population.
765 Can J Infect Dis Med Microbiol. 2007;18. doi:10.1155/2007/597123

766 6. Carré N, Sillam F, Dabas JP, Herbreteau N, Pinchon C, Ortmans C, et
767 al. Staphylococcus aureus carrying Panton-Valentine leukocidin
768 genes nasal colonization and skin infection: Screening in case of
769 outbreak in a school environment. Med Mal Infect. 2008;38.
770 doi:10.1016/j.medmal.2008.06.025

771 7. Carré N, Herbreteau N, Askeur N, Dabas JP, Pinchon C, Bes M, et al.
772 Outbreak of skin infections due to Staphylococcus aureus carrying
773 Panton-Valentine leukocidin genes in pupils and their relatives. Med
774 Mal Infect. 2011;41. doi:10.1016/j.medmal.2010.12.017

775 8. Higashiyama M, Ito T, Han X, Nishiyama J, Tanno A, Wada T, et al.
776 Trial to control an outbreak of Panton-Valentine leukocidin-positive
777 methicillin-resistant Staphylococcus aureus at a boarding school in
778 Japan. Am J Infect Control. 2011;39. doi:10.1016/j.ajic.2011.02.010

779 9. Bourigault C, Corvec S, Brulet V, Robert P-Y, Mounoury O, Goubin C,
780 et al. Outbreak of Skin Infections Due to Panton-Valentine
781 Leukocidin-Positive Methicillin-Susceptible Staphylococcus aureus in
782 a French Prison in 2010-2011. PLoS Curr. 2014.
783 doi:10.1371/currents.outbreaks.e4df88f057fc49e2560a235e0f8f9fea

784 10. Couvé-Deacon E, Tristan A, Pestourie N, Faure C, Doffoel-Hantz V,
785 Garnier F, et al. Outbreak of Panton-valentine leukocidin–associated
786 methicillin-susceptible staphylococcus aureus infection in a rugby
787 team, France, 2010–2011. Emerg Infect Dis. 2016;22.
788 doi:10.3201/eid2201.150597

789 11. Leistner R, Kola A, Gastmeier P, Krüger R, Hoppe P-A, Schneider-
790 Burrus S, et al. Pyoderma outbreak among kindergarten families:
791 Association with a Panton-Valentine leukocidin (PVL)-producing S.
792 aureus strain. Becker K, editor. PLoS One. 2017;12: e0189961.
793 doi:10.1371/journal.pone.0189961

794 12. Ismail H, Govender NP, Singh-Moodley A, Van Schalkwyk E, Shuping
795 L, Moema I, et al. An outbreak of cutaneous abscesses caused by
796 Panton-Valentine leukocidin-producing methicillin-susceptible
797 Staphylococcus aureus among gold mine workers, South Africa,
798 November 2017 to March 2018. BMC Infect Dis. 2020;20.
799 doi:10.1186/s12879-020-05352-5

800 13. Linde H, Wagenlehner F, Strommenger B, Drubel I, Tanzer J, Reischl
801 U, et al. Healthcare-associated outbreaks and community-acquired
802 infections due to MRSA carrying the Panton-Valentine leucocidin gene
803 in southeastern Germany. Eur J Clin Microbiol Infect Dis. 2005;24.
804 doi:10.1007/s10096-005-1341-7

805 14. Wagenlehner FME, Naber KG, Bambl E, Raab U, Wagenlehner C,
806 Kahlau D, et al. Management of a large healthcare-associated
807 outbreak of Panton-Valentine leucocidin-positive meticillin-resistant
808 Staphylococcus aureus in Germany. J Hosp Infect. 2007;67.
809 doi:10.1016/j.jhin.2007.07.006

810 15. Tang CT, Nguyen DT, Hoa NT, Nguyen TMP, Le VT, To SD, et al. An
811 outbreak of severe infections with community-acquired MRSA

812 carrying the panton-valentine leukocidin following vaccination. PLoS
813 One. 2007;2. doi:10.1371/journal.pone.0000822

814 16. Maltezou HC, Vourli S, Katerelos P, Maragos A, Kotsalidou S,
815 Remoudaki E, et al. Panton-Valentine leukocidin-positive methicillin-
816 resistant Staphylococcus aureus outbreak among healthcare workers
817 in a long-term care facility. Int J Infect Dis. 2009;13.
818 doi:10.1016/j.ijid.2009.02.004

819 17. Nagao M, Iinuma Y, Suzuki M, Matsushima A, Takakura S, Ito Y, et
820 al. First outbreak of methicillin-resistant Staphylococcus aureus
821 USA300 harboring the Panton-Valentine leukocidin genes among
822 Japanese health care workers and hospitalized patients. Am J Infect
823 Control. 2010;38. doi:10.1016/j.ajic.2010.04.214

824 18. Teare L, Shelley OP, Millership S, Kearns A. Outbreak of Panton-
825 Valentine leucocidin-positive meticillin-resistant Staphylococcus
826 aureus in a regional burns unit. J Hosp Infect. 2010;76.
827 doi:10.1016/j.jhin.2010.04.023

828 19. Ali H, Nash JQ, Kearns AM, Pichon B, Vasu V, Nixon Z, et al.
829 Outbreak of a South West Pacific clone Panton-Valentine leucocidin-
830 positive meticillin-resistant Staphylococcus aureus infection in a UK
831 neonatal intensive care unit. J Hosp Infect. 2012;80.
832 doi:10.1016/j.jhin.2011.12.019

833 20. Pinto AN, Seth R, Zhou F, Tallon J, Dempsey K, Tracy M, et al.
834 Emergence and control of an outbreak of infections due to Panton-

835 Valentine leukocidin positive, ST22 methicillin-resistant
836 Staphylococcus aureus in a neonatal intensive care unit. Clin
837 Microbiol Infect. 2013;19. doi:10.1111/j.1469-0691.2012.03987.x

838 21. Garvey MI, Bradley CW, Holden KL, Oppenheim B. Outbreak of clonal
839 complex 22 Panton–Valentine leucocidin-positive methicillin-resistant
840 Staphylococcus aureus. J Infect Prev. 2017;18.
841 doi:10.1177/1757177417695647

842 22. Kossow A, Kampmeier S, Schaumburg F, Knaack D, Moellers M,
843 Mellmann A. Whole genome sequencing reveals a prolonged and
844 spatially spread nosocomial outbreak of Panton–Valentine leucocidin-
845 positive meticillin-resistant Staphylococcus aureus (USA300). J Hosp
846 Infect. 2019;101. doi:10.1016/j.jhin.2018.09.007

847 23. Panigrahy A, Sinha S, Das BK, Kapil A, Vishnubhatla S, Dhawan B.
848 Staphylococcus aureus Colonisation in HIV-Infected Patients:
849 Incidence, Risk Factors and Subsequent Skin- and Soft-Tissue
850 Infections. Indian J Med Microbiol. 2020;38: 444–447.
851 doi:10.4103/ijmm.IJMM_20_5

852 24. Ikeuchi K, Adachi E, Sasaki T, Suzuki M, Lim LA, Saito M, et al. An
853 Outbreak of USA300 Methicillin-Resistant Staphylococcus aureus
854 Among People With HIV in Japan. J Infect Dis. 2021;223: 610–620.
855 doi:10.1093/infdis/jiaa651

856 25. Shallcross LJ, Fragaszy E, Johnson AM, Hayward AC. The role of the
857 Panton-Valentine leucocidin toxin in staphylococcal disease: A

858 systematic review and meta-analysis. Lancet Infect Dis. 2013;13.
859 doi:10.1016/S1473-3099(12)70238-4

860 26. Saeed K, Gould I, Espositio S, Ahmad-Saeed N, Ahmed SS, Alp E, et
861 al. Panton–Valentine leukocidin-positive Staphylococcus aureus: a
862 position statement from the International Society of Chemotherapy.
863 Int J Antimicrob Agents. 2018;51: 16–25.
864 doi:10.1016/j.ijantimicag.2017.11.002

865 27. Hoppe P-A, Holzhauer S, Lala B, Bührer C, Gratopp A, Hanitsch LG,
866 et al. Severe infections of Panton-Valentine leukocidin positive
867 Staphylococcus aureus in children. Medicine (Baltimore). 2019;98:
868 e17185. doi:10.1097/MD.0000000000017185

869 28. Rimoldi SG, Pileri P, Mazzocco MI, Romeri F, Bestetti G, Calvagna N,
870 et al. The Role of Staphylococcus aureus in Mastitis: A
871 Multidisciplinary Working Group Experience. J Hum Lact. 2020;36.
872 doi:10.1177/0890334419876272

873 29. Le Thomas I, Mariani-Kurkdjian P, Collignon A, Gravet A, Clermont
874 O, Brahimi N, et al. Breast milk transmission of a Panton-Valentine
875 leukocidin-producing Staphylococcus aureus strain causing infantile
876 pneumonia. J Clin Microbiol. 2001;39. doi:10.1128/JCM.39.2.728-
877 729.2001

878 30. Labandeira-Rey M, Couzon F, Boisset S, Brown EL, Bes M, Benito Y,
879 et al. Staphylococcus aureus Panton-Valentine leukocidin causes
880 necrotizing pneumonia. Science (80-). 2007;315.

881 doi:10.1126/science.1137165

882 31. Gillet Y, Issartel B, Vanhems P, Lina G, Vandenesch F, Etienne J, et
883 al. Severe staphylococcal pneumonia in children. Arch Pédiatrie.
884 2001;8. doi:10.1016/S0929-693X(01)80190-1

885 32. Li HT, Zhang TT, Huang J, Zhou YQ, Zhu JX, Wu BQ. Factors
886 associated with the outcome of life-threatening necrotizing
887 pneumonia due to community-acquired Staphylococcus aureus in
888 adult and adolescent patients. Respiration. 2011;81.
889 doi:10.1159/000319557

890 33. Duployez C, Le Guern R, Tinez C, Lejeune AL, Robriquet L, Six S, et
891 al. Panton-valentine leukocidin secreting staphylococcus aureus
892 pneumonia complicating COVID-19. Emerg Infect Dis. 2020;26:
893 1939–1941. doi:10.3201/eid2608.201413

894 34. Allou N, Allyn J, Traversier N, Baron M, Blondé R, Dupieux C, et al.
895 SARS-CoV-2 with Panton-Valentine leukocidin-producing
896 Staphylococcus aureus healthcare-associated pneumonia in the
897 Indian Ocean. Heliyon. 2022;8: e10422.
898 doi:10.1016/j.heliyon.2022.e10422

899 35. Nygaard U, Petersen A, Larsen AR, Rytter MJH, Hartling U, Kirkby N,
900 et al. Fatal SARS-CoV-2-Associated Panton-Valentine Leukocidin-
901 producing Staphylococcal Bacteremia: A Nationwide Multicenter
902 Cohort Study. Pediatr Infect Dis J. 2022;41: e142–e145.
903 doi:10.1097/INF.0000000000003476

904 36. Schaumburg F, Witten A, Flamen A, Stoll M, Alabi AS, Kremsner PG,
905 et al. Complement 5a Receptor Polymorphisms Are Associated With
906 Panton-Valentine Leukocidin–positive Staphylococcus aureus
907 Colonization in African Pygmies. Clin Infect Dis. 2018; 1–3.
908 doi:10.1093/cid/ciy666

909 37. Tromp AT, Van Gent M, Abrial P, Martin A, Jansen JP, De Haas CJC,
910 et al. Human CD45 is an f-component-specific receptor for the
911 staphylococcal toxin Panton-Valentine leukocidin. Nat Microbiol.
912 2018;3: 708–717. doi:10.1038/s41564-018-0159-x

913 38. Spaan AN, Henry T, Van Rooijen WJM, Perret M, Badiou C, Aerts PC,
914 et al. The staphylococcal toxin panton-valentine leukocidin targets
915 human C5a receptors. Cell Host Microbe. 2013;13: 584–594.
916 doi:10.1016/j.chom.2013.04.006

917 39. Alonzo F, Torres VJ. Bacterial Survival Amidst an Immune Onslaught:
918 The Contribution of the Staphylococcus aureus Leukotoxins. PLoS
919 Pathog. 2013;9: e1003143. doi:10.1371/journal.ppat.1003143

920 40. Spaan AN, Van Strijp JAG, Torres VJ. Leukocidins: Staphylococcal bi-
921 component pore-forming toxins find their receptors. Nat Rev
922 Microbiol. 2017;15: 435–447. doi:10.1038/nrmicro.2017.27

923 41. Holzinger D, Gieldon L, Mysore V, Nippe N, Taxman DJ, Duncan JA,
924 et al. Staphylococcus aureus Panton-Valentine leukocidin induces an
925 inflammatory response in human phagocytes via the NLRP3
926 inflammasome. J Leukoc Biol. 2012;92: 1069–1081.

927 doi:10.1189/jlb.0112014

928 42. van Kessel KPM, Bestebroer J, van Strijp JAG. Neutrophil-Mediated
929 Phagocytosis of Staphylococcus aureus. Front Immunol. 2014;5:
930 467. doi:10.3389/fimmu.2014.00467

931 43. Buvelot H, Posfay-Barbe KM, Linder P, Schrenzel J, Krause KH.
932 Staphylococcus aureus, phagocyte NADPH oxidase and chronic
933 granulomatous disease. FEMS Microbiol Rev. 2017;41.
934 doi:10.1093/femsre/fuw042

935 44. Brinkmann V, Reichard U, Goosmann C, Fauler B, Uhlemann Y, Weiss
936 DS, et al. Neutrophil extracellular traps kill bacteria. Science.
937 2004;303: 1532–5. doi:10.1126/science.1092385

938 45. Kenny EF, Herzig A, Krüger R, Muth A, Mondal S, Thompson PR, et
939 al. Diverse stimuli engage different neutrophil extracellular trap
940 pathways. Elife. 2017;6: e24437. doi:10.7554/eLife.24437

941 46. Fuchs TA, Abed U, Goosmann C, Hurwitz R, Schulze I, Wahn V, et al.
942 Novel cell death program leads to neutrophil extracellular traps. J
943 Cell Biol. 2007;176: 231–241. doi:10.1083/jcb.200606027

944 47. Papayannopoulos V, Metzler KD, Hakkim A, Zychlinsky A. Neutrophil
945 elastase and myeloperoxidase regulate the formation of neutrophil
946 extracellular traps. J Cell Biol. 2010;191: 677–691.
947 doi:10.1083/jcb.201006052

948 48. Sollberger G, Choidas A, Burn GL, Habenberger P, Di Lucrezia R,
949 Kordes S, et al. Gasdermin D plays a vital role in the generation of

950 neutrophil extracellular traps. Sci Immunol. 2018;3: eaar6689.
951 doi:10.1126/sciimmunol.aar6689

952 49. Pilsczek FH, Salina D, Poon KKH, Fahey C, Yipp BG, Sibley CD, et al.
953 A Novel Mechanism of Rapid Nuclear Neutrophil Extracellular Trap
954 Formation in Response to Staphylococcus aureus. J Immunol.
955 2010;185: 7413–7425. doi:10.4049/jimmunol.1000675

956 50. Bhattacharya M, Berends ETM, Chan R, Schwab E, Roy S, Sen CK, et
957 al. Staphylococcus aureus biofilms release leukocidins to elicit
958 extracellular trap formation and evade neutrophil-mediated killing.
959 Proc Natl Acad Sci U S A. 2018;115: 7416–7421.
960 doi:10.1073/pnas.1721949115

961 51. Mazzoleni V, Zimmermann-Meisse G, Smirnova A, Tarassov I,
962 Prévost G. Staphylococcus aureus Panton-Valentine Leukocidin
963 triggers an alternative NETosis process targeting mitochondria.
964 FASEB J. 2020; 1–22. doi:10.1096/fj.201902981R

965 52. Berends ETM, Horswill AR, Haste NM, Monestier M, Nizet V, Von
966 Köckritz-Blickwede M. Nuclease expression by Staphylococcus aureus
967 facilitates escape from neutrophil extracellular traps. J Innate
968 Immun. 2010;2: 576–586. doi:10.1159/000319909

969 53. Heyworth PG, Cross AR, Curnutte JT. Chronic granulomatous
970 disease. Curr Opin Immunol. 2003;15: 578–84. doi:10.1016/s0952-
971 7915(03)00109-2

972 54. Amulic B, Knackstedt SL, Abu Abed U, Deigendesch N, Harbort CJ,

973 Caffrey BE, et al. Cell-Cycle Proteins Control Production of Neutrophil
974 Extracellular Traps. Dev Cell. 2017;43: 449-462.e5.
975 doi:10.1016/j.devcel.2017.10.013

976 55. Sanders SA, Eisenthal R, Harrison R. NADH oxidase activity of human
977 xanthine oxidoreductase generation of superoxide anion. Eur J
978 Biochem. 1997;245: 541–548. doi:10.1111/j.1432-
979 1033.1997.00541.x

980 56. Li Y, Trush MA. Diphenyleneiodonium, an NAD(P)H oxidase inhibitor,
981 also potently inhibits mitochondrial reactive oxygen species
982 production. Biochem Biophys Res Commun. 1998;253: 295–299.
983 doi:10.1006/bbrc.1998.9729

984 57. Majander A, Finel M, Wikström M. Diphenyleneiodonium inhibits
985 reduction of iron-sulfur clusters in the mitochondrial NADH-
986 ubiquinone oxidoreductase (Complex I). J Biol Chem. 1994;269:
987 21037–21042. doi:10.1016/s0021-9258(17)31926-9

988 58. Galbusera C, Orth P, Fedida D, Spector T. Superoxide radical
989 production by allopurinol and xanthine oxidase. Biochem Pharmacol.
990 2006;71: 1747–52. doi:10.1016/j.bcp.2006.02.008

991 59. Metzler KD, Goosmann C, Lubojemska A, Zychlinsky A,
992 Papayannopoulos V. Myeloperoxidase-containing complex regulates
993 neutrophil elastase release and actin dynamics during NETosis. Cell
994 Rep. 2014;8: 883–896. doi:10.1016/j.celrep.2014.06.044

995 60. Petretto A, Bruschi M, Pratesi F, Croia C, Candiano G, Ghiggeri G, et

996 al. Neutrophil extracellular traps (NET) induced by different stimuli:
997 A comparative proteomic analysis. PLoS One. 2019;14: 1–18.
998 doi:10.1371/journal.pone.0218946

999 61. Scola AM, Johswich KO, Morgan BP, Klos A, Monk PN. The human
1000 complement fragment receptor, C5L2, is a recycling decoy receptor.
1001 Mol Immunol. 2009;46: 1149–1162.
1002 doi:10.1016/j.molimm.2008.11.001

1003 62. Bamberg CE, Mackay CR, Lee H, Zahra D, Jackson J, Lim YS, et al.
1004 The C5a receptor (C5aR) C5L2 is a modulator of C5aR-mediated
1005 signal transduction. J Biol Chem. 2010;285: 7633–7644.
1006 doi:10.1074/jbc.M109.092106

1007 63. Genestier A-L, Michallet M-C, Prévost G, Bellot G, Chalabreysse L,
1008 Peyrol S, et al. Staphylococcus aureus Panton-Valentine leukocidin
1009 directly targets mitochondria and induces Bax-independent apoptosis
1010 of human neutrophils. J Clin Invest. 2005;115: 3117–3127.
1011 doi:10.1172/JCI22684

1012 64. Badiou C, Dumitrescu O, George N, Forbes ARN, Drougka E, Chan
1013 KS, et al. Rapid detection of Staphylococcus aureus Panton-Valentine
1014 Leukocidin in clinical specimens by enzyme-linked immunosorbent
1015 assay and immunochromatographic tests. J Clin Microbiol. 2010;48:
1016 1384–1390. doi:10.1128/JCM.02274-09

1017 65. Fuchs TA, Brill A, Duerschmied D, Schatzberg D, Monestier M, Myers
1018 DD, et al. Extracellular DNA traps promote thrombosis. Proc Natl

1019 Acad Sci U S A. 2010;107: 15880–15885.
1020 doi:10.1073/pnas.1005743107

1021 66. Kahlenberg JM, Carmona-Rivera C, Smith CK, Kaplan MJ. Neutrophil
1022 extracellular trap-associated protein activation of the NLRP3
1023 inflammasome is enhanced in lupus macrophages. J Immunol.
1024 2013;190: 1217–26. doi:10.4049/jimmunol.1202388

1025 67. Apel F, Andreeva L, Knackstedt LS, Streeck R, Frese CK, Goosmann
1026 C, et al. The cytosolic DNA sensor cGAS recognizes neutrophil
1027 extracellular traps. Sci Signal. 2021;14: eaax7942.
1028 doi:10.1126/scisignal.aax7942

1029 68. Losman MJ, Fasy TM, Novick KE, Monestier M. Monoclonal
1030 autoantibodies to subnucleosomes from a MRL/Mp(-)+/+ mouse.
1031 Oligoclonality of the antibody response and recognition of a
1032 determinant composed of histones H2A, H2B, and DNA. J Immunol.
1033 1992;148: 1561–9. Available:
1034 http://www.ncbi.nlm.nih.gov/pubmed/1371530

1035 69. Hughes CS, Moggridge S, Müller T, Sorensen PH, Morin GB,
1036 Krijgsveld J. Single-pot, solid-phase-enhanced sample preparation
1037 for proteomics experiments. Nat Protoc. 2019;14: 68–85.
1038 doi:10.1038/s41596-018-0082-x

1039 70. Plubell DL, Wilmarth PA, Zhao Y, Fenton AM, Minnier J, Reddy AP, et
1040 al. Extended Multiplexing of Tandem Mass Tags (TMT) Labeling
1041 Reveals Age and High Fat Diet Specific Proteome Changes in Mouse

1042 Epididymal Adipose Tissue. Mol Cell Proteomics. 2017;16: 873–890.
1043 doi:10.1074/mcp.M116.065524

1044 71. Robinson MD, McCarthy DJ, Smyth GK. edgeR: a Bioconductor
1045 package for differential expression analysis of digital gene expression
1046 data. Bioinformatics. 2010;26: 139–140.
1047 doi:10.1093/BIOINFORMATICS/BTP616

1048 72. Ritchie ME, Phipson B, Wu D, Hu Y, Law CW, Shi W, et al. limma
1049 powers differential expression analyses for RNA-sequencing and
1050 microarray studies. Nucleic Acids Res. 2015;43: e47–e47.
1051 doi:10.1093/nar/gkv007

1052 73. Kammers K, Cole RN, Tiengwe C, Ruczinski I. Detecting Significant
1053 Changes in Protein Abundance. EuPA open proteomics. 2015;7: 11–
1054 19. doi:10.1016/j.euprot.2015.02.002

1055 74. Larsson J. eulerr: Area-Proportional Euler and Venn Diagrams with
1056 Ellipses. R package version 6.1.1. 2021. Available: https://cran.r-
1057 project.org/package=eulerr

1058 75. Kolde R. pheatmap: Pretty Heatmaps. R package version 1.0.12.
1059 2019.

1060 76. Perez-Riverol Y, Csordas A, Bai J, Bernal-Llinares M, Hewapathirana
1061 S, Kundu DJ, et al. The PRIDE database and related tools and
1062 resources in 2019: improving support for quantification data. Nucleic
1063 Acids Res. 2019;47: D442–D450. doi:10.1093/nar/gky1106

1064

1065

1066 **Supplemental Figures**

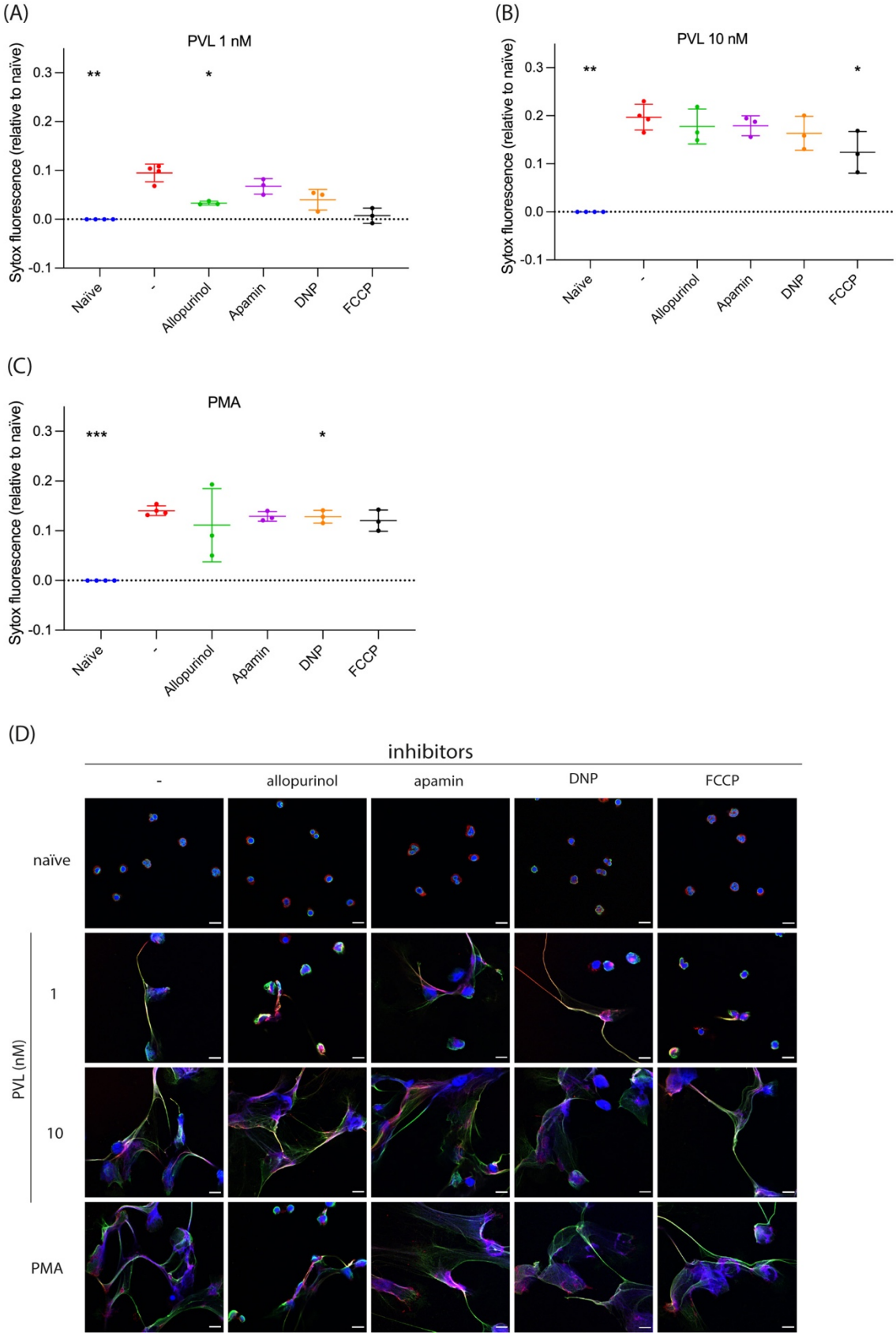

1084 **S1 Fig. FCCP and allopurinol inhibit PVL-induced NET formation.**

1085 Human primary neutrophils were treated with xanthine oxidase inhibitor

1086 allopurinol (2 mM), small conductance calcium-activated potassium
1087 channel inhibitor apamin (200 nM), and mitochondrial uncouplers DNP
1088 (750 μM) and FCCP (10 μM) for 30 min before stimulating with (A) PVL 1
1089 nM, (B) PVL 10 nM or (C) PMA for 4 h. We quantified cell death using
1090 SYTOX Green and fluorescence relative to naïve is plotted for the
1091 respective stimuli. (D) Representative confocal microscopy of naïve
1092 neutrophils or after stimulation with PMA or PVL in the presence or
1093 absence of indicated inhibitors, and stained for DNA (blue), NE (red) and
1094 chromatin (green). Scale bar represents 10 μm. (A-C) Mean ± SD of three
1095 independent experiments. *$P<0.05$, ** $P<0.01$, *** $P<0.001$ mixed-
1096 effects analysis with Dunnett´s multiple comparison test.

1097

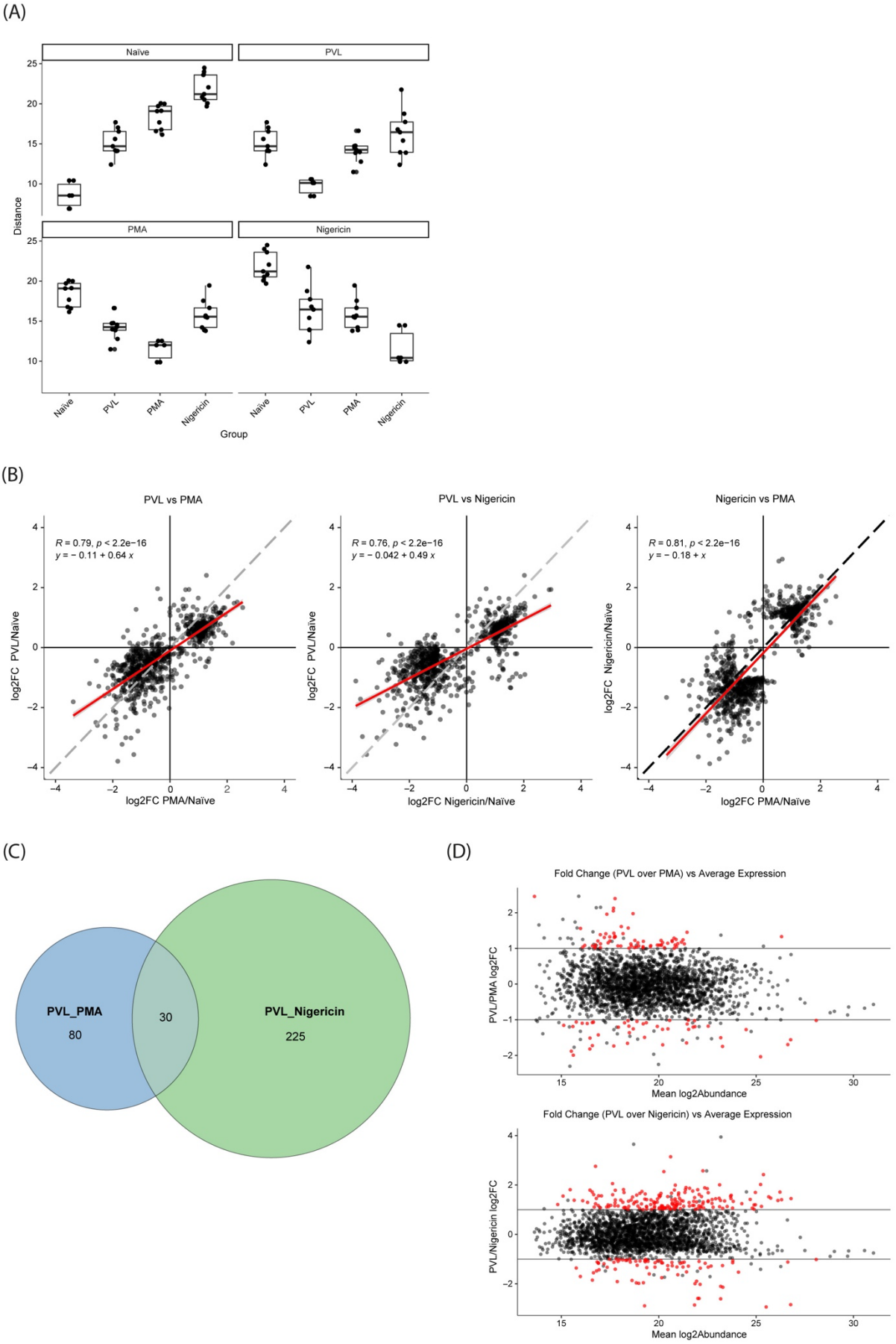

S2 Fig. Comparison of PVL, PMA, and nigericin NET proteomes. (A)

1100 Euclidean distance between whole proteomes of naïve neutrophils and
1101 NETs induced by different stimuli. For each panel, the pairwise distance is
1102 plotted between each sample of that group and the samples of the group
1103 indicated on the x-axis. Each point represents the distance between a
1104 unique pair of samples. (B) Scatter plots of DAP fold changes compared to
1105 naïve neutrophils with linear regression for PVL vs PMA NETs, PVL vs
1106 nigericin NETs, and nigericin vs PMA NETs. DAPs plotted are proteins
1107 significantly enriched or depleted in one or more NET groups compared to
1108 naïve neutrophils (as in Fig 3B and 3C). (C) Protein log2 fold change in
1109 PVL/PMA NETs or PVL/nigericin NETs vs mean abundance across samples.
1110 Data are from pairwise comparisons between PVL and PMA or PVL and
1111 nigericin NETs. Proteome data are from n=3 donors for each condition.
1112 Significant DAPs are colored red. DAPs from each indicated comparison
1113 were considered significant with an absolute log2 fold change > 1 and
1114 adjusted *p* value < 0.01.

1115

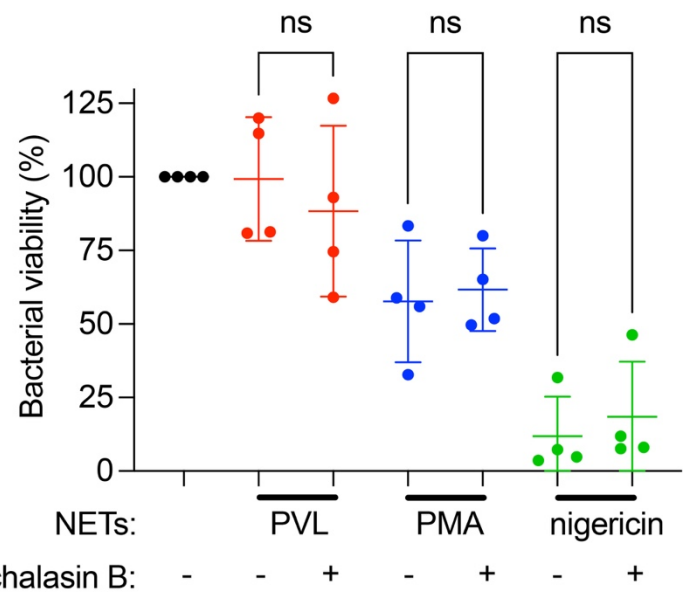

S3 Fig. Inhibition of phagocytosis by cytochalasin B does not affect killing by NETs

NET formation was induced by PVL (100 nM), PMA (100 nM), or nigericin (30 μM) for 4 h, followed by incubation with cytochalasin B (10 μg/ml) for 15 min. MRSA was incubated with the NETs for 1 h and CFUs were quantified after overnight incubation on TSA plates. Results are expressed as a percentage of CFUs formed by MRSA incubated in the absence of NETs.

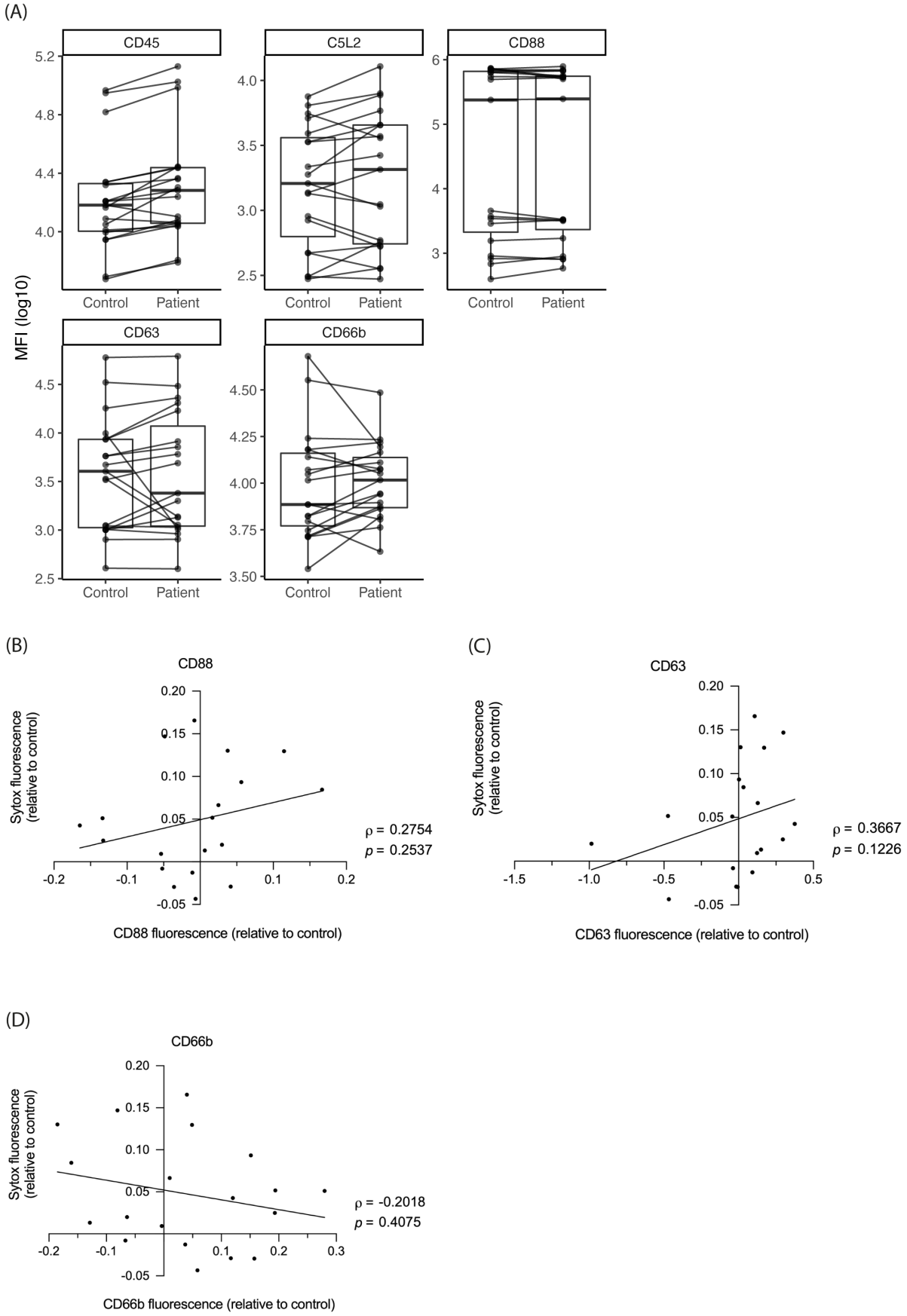

S4 Fig. Comparison of receptor expression between patients and controls and correlation with cell death. (A) Pair-wise comparison of

1130 CD45, C5L2, CD88, CD63, and CD66b MFI between patients and controls.
1131 (B-D) CD88, CD63, and CD66b fluorescence relative to control was plotted
1132 against SYTOX Green fluorescence induced by 0.1 nM PVL relative to
1133 control. The coefficient of correlation (ρ) and probability (p) of a
1134 Spearman's correlation test are indicated. A best-fit line indicates the
1135 trend.

1136 **S1-8 movies**

1137 Live cell imaging of control or CGD neutrophils left untreated (S1 and S5)
1138 or stimulated with 50 nM PMA (S2 and S6) or 1 nM PVL (S3-S4 and S7-
1139 S8) over a time course of 6 h. Images were acquired every 2 min. Cells
1140 were stained with the cell permeable DNA dye DRAQ5 (magenta) and the
1141 cell impermeable DNA dye SYTOX Green (green).

1142

1143 **List of abbreviations**

1144 CFU Colony forming unit

1145 CGD Chronic granulomatous disease

1146 DAP Differentially abundant proteins

1147 DAPI 4´,6-diamidino-2-phenylindole

1148 DHR Dihydrorhodamine

1149 DNP Dinitrophenol

1150 DPBS Dulbeccos`s phosphate-buffered saline

1151 DPI Diphenyleneiodonium chloride

1152 FCCP Carbonyl cyanide-p-trifluoromethoxyphenylhydrazone

1153 FDR False discovery rate

1154 HCD Higher-energy collisional dissociation

1155 HEPES Hydroxyethyl-Piperazine-Ethane Sulfonic Acid

1156 Hlg γ-Hemolysin

1157 HAS Human serum albumin

1158 MFI Mean fluorescent intensities

1159 MPO Myeloperoxidase

1160 MRSA Methicillin-resistant *Staphylococcus aureus*

1161 MS Mass spectrometry

1162 NE Neutrophil elastase

1163 NEi Neutrophil elastase inhibitor

1164 NETs Neutrophil extracellular traps

1165 PBS Phosphate-buffered saline

1166 PFA Paraformaldehyde

1167 PKC Protein Kinase C

1168 PMA Phorbol 12-myristate 13-acetate

1169 PMN Polymorphonuclear leukocytes

1170	PSMs	Peptide-spectrum-matches
1171	PVL	Panton-Valentine leukocidin
1172	PVL-SA	PVL-positive *S. aureus*
1173	ROS	Reactive oxygen species
1174	RT	Room temperature
1175	*S. aureus*	*Staphylococcus aureus*
1176	SDS	Sodium Dodecyl Sulfate
1177	SSTI	Skin and soft tissue infections
1178	TCEP	Tris-(2-carboxyethyl)phosphine
1179	TFA	Trifluoroacetic acid
1180	TMM	Trimmed mean of M values
1181	TMT	Tandem Mass Tag